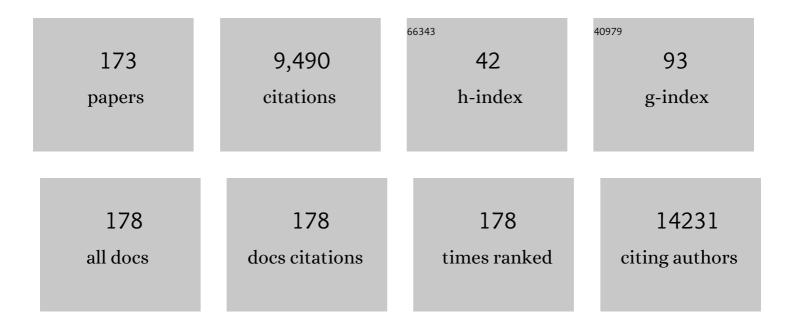
## Jaebeom Lee

List of Publications by Year in descending order

Source: https://exaly.com/author-pdf/4580185/publications.pdf Version: 2024-02-01



INFREOM LEE

#	Article	IF	CITATIONS
1	Nanoscale hydroxyapatite particles for bone tissue engineering. Acta Biomaterialia, 2011, 7, 2769-2781.	8.3	1,236
2	Gold nanoparticle ensembles as heaters and actuators: melting and collective plasmon resonances. Nanoscale Research Letters, 2006, 1, 84-90.	5.7	582
3	Excitonâ~'Plasmon Interaction and Hybrid Excitons in Semiconductorâ~'Metal Nanoparticle Assemblies. Nano Letters, 2006, 6, 984-994.	9.1	482
4	Bioconjugates of CdTe Nanowires and Au Nanoparticles:Â Plasmonâ^'Exciton Interactions, Luminescence Enhancement, and Collective Effects. Nano Letters, 2004, 4, 2323-2330.	9.1	364
5	Light-Controlled Self-Assembly of Semiconductor Nanoparticles into Twisted Ribbons. Science, 2010, 327, 1355-1359.	12.6	341
6	Exciton–plasmon interactions in molecular spring assemblies of nanowires and wavelength-based protein detection. Nature Materials, 2007, 6, 291-295.	27.5	315
7	Chiral Graphene Quantum Dots. ACS Nano, 2016, 10, 1744-1755.	14.6	304
8	Various preparation methods of highly porous hydroxyapatite/polymer nanoscale biocomposites for bone regeneration. Acta Biomaterialia, 2011, 7, 3813-3828.	8.3	258
9	Layer-by-Layer Assembly of Nacre-like Nanostructured Composites with Antimicrobial Properties. Langmuir, 2005, 21, 11915-11921.	3.5	239
10	Theory of plasmon-enhanced Förster energy transfer in optically excited semiconductor and metal nanoparticles. Physical Review B, 2007, 76, .	3.2	238
11	Exponential Growth of LBL Films with Incorporated Inorganic Sheets. Nano Letters, 2008, 8, 1762-1770.	9.1	210
12	Nanoparticle Assemblies with Molecular Springs: A Nanoscale Thermometer. Angewandte Chemie - International Edition, 2005, 44, 7439-7442.	13.8	188
13	Silver Nanowire Embedded in P3HT:PCBM for High-Efficiency Hybrid Photovoltaic Device Applications. ACS Nano, 2011, 5, 3319-3325.	14.6	184
14	Thermometer design at the nanoscale. Nano Today, 2007, 2, 48-51.	11.9	179
15	Layer-by-Layer Assembled Films of Cellulose Nanowires with Antireflective Properties. Langmuir, 2007, 23, 7901-7906.	3.5	165
16	Bioconjugated Superstructures of CdTe Nanowires and Nanoparticles: Multistep Cascade Förster Resonance Energy Transfer and Energy Channeling. Nano Letters, 2005, 5, 2063-2069.	9.1	157
17	Wrinkled Surface-Mediated Antibacterial Activity of Graphene Oxide Nanosheets. ACS Applied Materials & Interfaces, 2017, 9, 1343-1351.	8.0	154
18	Magnetic Nanozyme-Linked Immunosorbent Assay for Ultrasensitive Influenza A Virus Detection. ACS Applied Materials & Interfaces, 2018, 10, 12534-12543.	8.0	144

#	Article	IF	CITATIONS
19	Bioconjugated Ag Nanoparticles and CdTe Nanowires: Metamaterials with Field-Enhanced Light Absorption. Angewandte Chemie - International Edition, 2006, 45, 4819-4823.	13.8	112
20	Enhanced catalytic activity of gold nanoparticle-carbon nanotube hybrids for influenza virus detection. Biosensors and Bioelectronics, 2016, 85, 503-508.	10.1	103
21	In situ self-assembly of gold nanoparticles on hydrophilic and hydrophobic substrates for influenza virus-sensing platform. Scientific Reports, 2017, 7, 44495.	3.3	97
22	Dual-Mode SERS-Fluorescence Immunoassay Using Graphene Quantum Dot Labeling on One-Dimensional Aligned Magnetoplasmonic Nanoparticles. ACS Applied Materials & Interfaces, 2015, 7, 12168-12175.	8.0	95
23	A plasmon-assisted fluoro-immunoassay using gold nanoparticle-decorated carbon nanotubes for monitoring the influenza virus. Biosensors and Bioelectronics, 2015, 64, 311-317.	10.1	90
24	Green synthesis of phytochemical-stabilized Au nanoparticles under ambient conditions and their biocompatibility and antioxidative activity. Journal of Materials Chemistry, 2011, 21, 13316.	6.7	84
25	Ultrasensitive DNA monitoring by Au–Fe3O4 nanocomplex. Sensors and Actuators B: Chemical, 2012, 163, 224-232.	7.8	76
26	Detection of influenza virus using peroxidaseâ€mimic of gold nanoparticles. Biotechnology and Bioengineering, 2016, 113, 2298-2303.	3.3	72
27	Selfâ€Assembly Mechanism of Spiky Magnetoplasmonic Supraparticles. Advanced Functional Materials, 2014, 24, 1439-1448.	14.9	70
28	Chiral zirconium quantum dots: A new class of nanocrystals for optical detection of coronavirus. Heliyon, 2018, 4, e00766.	3.2	69
29	Electrochemical immunosensor using nanotriplex of graphene quantum dots, Fe3O4, and Ag nanoparticles for tuberculosis. Electrochimica Acta, 2018, 290, 369-377.	5.2	67
30	Accelerated healing of cutaneous wounds using phytochemically stabilized gold nanoparticle deposited hydrocolloid membranes. Biomaterials Science, 2015, 3, 509-519.	5.4	64
31	Potassium ion sensing using a self-assembled calix[4]crown monolayer by surface plasmon resonance. Sensors and Actuators B: Chemical, 2008, 133, 577-581.	7.8	63
32	Surface plasmon resonance spectroscopic characterization of antibody orientation and activity on the calixarene monolayer. Sensors and Actuators B: Chemical, 2010, 147, 548-553.	7.8	60
33	Folic acid–conjugated chitosan-functionalized graphene oxide for highly efficient photoacoustic imaging-guided tumor-targeted photothermal therapy. International Journal of Biological Macromolecules, 2020, 155, 961-971.	7.5	60
34	Difference between Toxicities of Iron Oxide Magnetic Nanoparticles with Various Surface-Functional Groups against Human Normal Fibroblasts and Fibrosarcoma Cells. Materials, 2013, 6, 4689-4706.	2.9	51
35	Magnetoplasmonic Nanomaterials for Biosensing/Imaging and <i>in Vitro</i> / <i>in Vivo</i> Biousability. Analytical Chemistry, 2018, 90, 225-239.	6.5	51
36	Scalable Solvothermal Synthesis of Superparamagnetic Fe <sub>3</sub> O <sub>4</sub> Nanoclusters for Bioseparation and Theragnostic Probes. ACS Applied Materials & Interfaces, 2018, 10, 41935-41946.	8.0	51

#	Article	IF	CITATIONS
37	Plasmon-Induced Photoluminescence Immunoassay for Tuberculosis Monitoring Using Gold-Nanoparticle-Decorated Graphene. ACS Applied Materials & Interfaces, 2014, 6, 21380-21388.	8.0	49
38	An easy and sensitive sandwich assay for detection of Mycobacterium tuberculosis Ag85B antigen using quantum dots and gold nanorods. Biosensors and Bioelectronics, 2017, 87, 150-156.	10.1	49
39	Ultrasensitive immunosensing of tuberculosis CFP-10 based on SPR spectroscopy. Sensors and Actuators B: Chemical, 2011, 156, 271-275.	7.8	46
40	Non-toxic nanoparticles from phytochemicals: preparation and biomedical application. Bioprocess and Biosystems Engineering, 2014, 37, 983-989.	3.4	46
41	Metal enhanced fluorescence on nanoporous gold leaf-based assay platform for virus detection. Biosensors and Bioelectronics, 2014, 58, 33-39.	10.1	44
42	Magneto-plamonic nanoparticles enhanced surface plasmon resonance TB sensor based on recombinant gold binding antibody. Sensors and Actuators B: Chemical, 2017, 250, 356-363.	7.8	43
43	Helical Magnetic Field-Induced Real-Time Plasmonic Chirality Modulation. ACS Nano, 2020, 14, 7152-7160.	14.6	43
44	Media Effect on CdTe Nanowire Growth:  Mechanism of Self-Assembly, Ostwald Ripening, and Control of NW Geometry. Journal of Physical Chemistry C, 2008, 112, 370-377.	3.1	42
45	Functionalization Effects of Single-Walled Carbon Nanotubes as Templates for the Synthesis of Silica Nanorods and Study of Growing Mechanism of Silica. ACS Nano, 2010, 4, 3933-3942.	14.6	42
46	Phase-Pure FeSe <sub><i>x</i></sub> ( <i>x</i> = 1, 2) Nanoparticles with One- and Two-Photon Luminescence. Journal of the American Chemical Society, 2014, 136, 7189-7192.	13.7	41
47	Early detection of the growth of Mycobacterium tuberculosis using magnetophoretic immunoassay in liquid culture. Biosensors and Bioelectronics, 2017, 96, 68-76.	10.1	41
48	Synthesis of Length-Controlled Aerosol Carbon Nanotubes and Their Dispersion Stability in Aqueous Solution. Langmuir, 2009, 25, 1739-1743.	3.5	39
49	Multifunctional Magnetoplasmonic Nanomaterials and Their Biomedical Applications. Journal of Biomedical Nanotechnology, 2014, 10, 2921-2949.	1.1	38
50	Transdermal treatment of the surgical and burned wound skin via phytochemical-capped gold nanoparticles. Colloids and Surfaces B: Biointerfaces, 2015, 135, 166-174.	5.0	38
51	Recent tuberculosis diagnosis toward the end TB strategy. Journal of Microbiological Methods, 2016, 123, 51-61.	1.6	38
52	Cancer upregulated gene 2 induces epithelial-mesenchymal transition of human lung cancer cells via TGF-β signaling. Oncotarget, 2017, 8, 5092-5110.	1.8	37
53	Mechanical properties of multilayered chitosan/CNT nanocomposite films. Materials Science & Engineering A: Structural Materials: Properties, Microstructure and Processing, 2011, 528, 6636-6641.	5.6	36
54	Magnetic-Field-Induced Electrochemical Performance of a Porous Magnetoplasmonic Ag@Fe <sub>3</sub> O <sub>4</sub> Nanoassembly. ACS Applied Materials & Interfaces, 2020, 12, 6598-6606.	8.0	36

#	Article	IF	CITATIONS
55	Preparation of multi-layered film of hydroxyapatite and chitosan. Materials Science and Engineering C, 2010, 30, 789-794.	7.3	33
56	Rapid monitoring of CFP-10 during culture of Mycobacterium tuberculosis by using a magnetophoretic immunoassay. Sensors and Actuators B: Chemical, 2013, 177, 327-333.	7.8	32
57	Hyaluronic Acid/Poly(lactic- <i>co</i> -glycolic acid) Core/Shell Fiber Meshes Loaded with Epigallocatechin-3- <i>O</i> -Gallate as Skin Tissue Engineering Scaffolds. Journal of Nanoscience and Nanotechnology, 2014, 14, 8458-8463.	0.9	32
58	Molecular Recognition of Arginine by Supramolecular Complexation with Calixarene Crown Ether Based on Surface Plasmon Resonance. International Journal of Molecular Sciences, 2011, 12, 2315-2324.	4.1	31
59	Metal nanowire percolation micro-grids embedded in elastomers for stretchable and transparent conductors. Journal of Materials Chemistry C, 2015, 3, 8241-8247.	5.5	31
60	Synthesis and formation mechanism of bone mineral, whitlockite nanocrystals in tri-solvent system. Journal of Colloid and Interface Science, 2020, 569, 1-11.	9.4	31
61	Quantum dots incorporated magnetic nanoparticles for imaging colon carcinoma cells. Journal of Nanobiotechnology, 2013, 11, 28.	9.1	30
62	Simple and Cost-Effective Fabrication of Highly Flexible, Transparent Superhydrophobic Films with Hierarchical Surface Design. ACS Applied Materials & Interfaces, 2015, 7, 5289-5295.	8.0	30
63	Small molecule induced self-assembly of Au nanoparticles. Journal of Materials Chemistry, 2011, 21, 16935.	6.7	29
64	Plastic-Chip-Based Magnetophoretic Immunoassay for Point-of-Care Diagnosis of Tuberculosis. ACS Applied Materials & Interfaces, 2016, 8, 23489-23497.	8.0	29
65	Tuning Plasmon Resonance in Magnetoplasmonic Nanochains by Controlling Polarization and Interparticle Distance for Simple Preparation of Optical Filters. ACS Applied Materials & Interfaces, 2017, 9, 24433-24439.	8.0	29
66	N-doped microporous carbon hollow spheres with precisely controlled architectures for supercapacitor. Electrochimica Acta, 2019, 313, 389-396.	5.2	28
67	Clinical immunosensing of tuberculosis CFP-10 in patient urine by surface plasmon resonance spectroscopy. Sensors and Actuators B: Chemical, 2011, 160, 1434-1438.	7.8	27
68	Rapid detection of DNA by magnetophoretic assay. Sensors and Actuators B: Chemical, 2014, 198, 77-81.	7.8	26
69	Metal-Enhanced Fluorescence: Wavelength-Dependent Ultrafast Energy Transfer. Journal of Physical Chemistry C, 2015, 119, 23285-23291.	3.1	26
70	Control of Energy Transfer to CdTe Nanowires via Conjugated Polymer Orientation. Journal of Physical Chemistry C, 2009, 113, 109-116.	3.1	25
71	Sensitive detection of tuberculosis using nanoparticle-enhanced surface plasmon resonance. Mikrochimica Acta, 2013, 180, 431-436.	5.0	25
72	Visual determination of aliphatic diamines based on host–guest recognition of calix[4]arene derivatives capped gold nanoparticles. Biosensors and Bioelectronics, 2015, 72, 306-312.	10.1	25

#	Article	IF	CITATIONS
73	Self-assembled magnetoplasmonic nanochain for DNA sensing. Sensors and Actuators B: Chemical, 2014, 203, 817-823.	7.8	24
74	Transition Metal-Based 2D Layered Double Hydroxide Nanosheets: Design Strategies and Applications in Oxygen Evolution Reaction. Nanomaterials, 2021, 11, 1388.	4.1	24
75	Controlled thin layer coating of carbon nanotube-polymer composites for UV-visible light protection. Korean Journal of Chemical Engineering, 2009, 26, 1790-1794.	2.7	23
76	Preparation of concave magnetoplasmonic core-shell supraparticles of gold-coated iron oxide via ion-reducible layer-by-layer method for surface enhanced Raman scattering. Journal of Colloid and Interface Science, 2017, 499, 54-61.	9.4	23
77	Emission-tunable probes using terbium(III)-doped self-activated luminescent hydroxyapatite for in vitro bioimaging. Journal of Colloid and Interface Science, 2021, 581, 21-30.	9.4	23
78	Preparation of High Flexible Composite Film of Hydroxyapatite and Chitosan. Polymer Bulletin, 2009, 62, 111-118.	3.3	22
79	Photoluminescence enhancement of quantum dots on Ag nanoneedles. Nanoscale Research Letters, 2012, 7, 438.	5.7	22
80	Magnetic-Assembly Mechanism of Superparamagneto-Plasmonic Nanoparticles on a Charged Surface. ACS Applied Materials & Interfaces, 2015, 7, 8650-8658.	8.0	22
81	Synthesis of Gold Nanoparticles with Buffer-Dependent Variations of Size and Morphology in Biological Buffers. Nanoscale Research Letters, 2016, 11, 65.	5.7	22
82	Magnetic field-aligned Fe3O4-coated silver magnetoplasmonic nanochain with enhanced sensitivity for detection of Siglec-15. Biosensors and Bioelectronics, 2021, 191, 113448.	10.1	20
83	In-Vivo and In-Vitro Biocompatibility Evaluations of Silver Nanoparticles with Antimicrobial Activity. Journal of Nanoscience and Nanotechnology, 2012, 12, 5205-5209.	0.9	19
84	3D hierarchically porous magnetic molybdenum trioxide@gold nanospheres as a nanogap-enhanced Raman scattering biosensor for SARS-CoV-2. Nanoscale Advances, 2022, 4, 871-883.	4.6	19
85	Synthesis and characterization of gold-deposited red, green and blue fluorescent silica nanoparticles for biosensor application. Chemical Communications, 2010, 46, 6374.	4.1	18
86	<i>In vivo</i> study on the biocompatibility of chitosan–hydroxyapatite film depending on degree of deacetylation. Journal of Biomedical Materials Research - Part A, 2017, 105, 1637-1645.	4.0	18
87	Influence of ultrasonication on the mechanical properties of Cu/Al2O3 nanocomposite thin films during electrocodeposition. Surface and Coatings Technology, 2010, 205, 2362-2368.	4.8	17
88	Surface-plasmon-assisted modal gain enhancement in Au-hybrid CdSe/ZnS nanocrystal quantum dots. Applied Physics Letters, 2011, 99, .	3.3	17
89	Cytotoxicity and Gene Expression in Sarcoma 180 Cells in Response to Spiky Magnetoplasmonic Supraparticles. ACS Applied Materials & Interfaces, 2014, 6, 19680-19689.	8.0	17
90	Scalable and inexpensive strategy to fabricate CuO/ZnO nanowire heterojunction for efficient photoinduced water splitting. Journal of Materials Science, 2018, 53, 2725-2734.	3.7	17

#	Article	IF	CITATIONS
91	Biocompatibility of Nanoscale Hydroxyapatite-embedded Chitosan Films. Bulletin of the Korean Chemical Society, 2012, 33, 3950-3956.	1.9	17
92	Rapid Assembly of Magnetoplasmonic Photonic Arrays for Brilliant, Noniridescent, and Stimuliâ€Responsive Structural Colors. Small, 2022, 18, e2200317.	10.0	17
93	Magnetically recyclable catalytic activity of spiky magneto-plasmonic nanoparticles. RSC Advances, 2015, 5, 56653-56657.	3.6	16
94	Synthesis Mechanism of Magnetite Nanorods Containing Ordered Mesocages. Chemistry of Materials, 2019, 31, 2263-2268.	6.7	16
95	Clinical Trial: Magnetoplasmonic ELISA for Urine-based Active Tuberculosis Detection and Anti-Tuberculosis Therapy Monitoring. ACS Central Science, 2021, 7, 1898-1907.	11.3	16
96	Aptamer-Assisted Protein Orientation on Silver Magnetic Nanoparticles: Application to Sensitive Leukocyte Cell-Derived Chemotaxin 2 Surface Plasmon Resonance Sensors. Analytical Chemistry, 2022, 94, 2109-2118.	6.5	16
97	Fe-based multifunctional nanoparticles with various physicochemical properties. Current Applied Physics, 2017, 17, 1066-1078.	2.4	15
98	Feâ€Based Mesoporous Nanostructures for Electrochemical Conversion and Storage of Energy. Batteries and Supercaps, 2021, 4, 429-444.	4.7	15
99	One-Pot Synthesis of Magnetoplasmonic Au@Fe <sub><i>x</i></sub> O <sub><i>y</i></sub> Nanowires: Bioinspired Bouligand Chiral Stack. ACS Nano, 2022, 16, 5795-5806.	14.6	15
100	Building a novel vitronectin assay by immobilization of integrin on calixarene monolayer. Talanta, 2007, 75, 99-103.	5.5	14
101	Guided Bone Regeneration Using a Flexible Hydroxyapatite Patch. Journal of Biomedical Nanotechnology, 2013, 9, 1914-1920.	1.1	14
102	Enhancement of primary neuronal cell proliferation using printingâ€ŧransferred carbon nanotube sheets. Journal of Biomedical Materials Research - Part A, 2015, 103, 1746-1754.	4.0	14
103	Synthesis of silver nanoparticles using analogous reducibility of phytochemicals. Current Applied Physics, 2016, 16, 738-747.	2.4	14
104	Magneto-optically active magnetoplasmonic graphene. Chemical Communications, 2017, 53, 5814-5817.	4.1	14
105	Colorimetric Detection of <i>Mycobacterium tuberculosis</i> ESX-1 Substrate Protein in Clinical Samples Using Au@Pd Nanoparticle-Based Magnetic Enzyme-Linked Immunosorbent Assay. ACS Applied Nano Materials, 2021, 4, 539-549.	5.0	14
106	Hydroxyapatite coating on damaged tooth surfaces by immersion. Biomedical Materials (Bristol), 2009, 4, 025017.	3.3	13
107	Comparative SPR study on the effect of nanomaterials on the biological activity of adsorbed proteins. Mikrochimica Acta, 2012, 178, 301-307.	5.0	13
108	Fabrication of large area flexible and highly transparent film by a simple Ag nanowire alignment. Journal of Experimental Nanoscience, 2013, 8, 130-137.	2.4	13

#	Article	IF	CITATIONS
109	Plasmonic Enhancement of Chiroptical Property in Enantiomers Using a Helical Array of Magnetoplasmonic Nanoparticles for Ultrasensitive Chiral Recognition. ACS Applied Materials & Interfaces, 2021, 13, 46886-46893.	8.0	13
110	Gold nanoparticles with stable yellow-green luminescence. International Journal of Nanotechnology, 2007, 4, 239.	0.2	12
111	Development of surface plasmon resonance immunosensor for the novel protein immunostimulating factor. Mikrochimica Acta, 2011, 172, 171-176.	5.0	12
112	Building a sensitive immunosensing platform based on oriented immobilization of histidine-tagged antibody on NiO-decorated SWNTs. Sensors and Actuators B: Chemical, 2013, 181, 38-43.	7.8	12
113	Clinical immunosensing of tuberculosis CFP-10 antigen in urine using interferometric optical fiber array. Sensors and Actuators B: Chemical, 2015, 216, 184-191.	7.8	12
114	Whitlockite Granules on Bone Regeneration in Defect of Rat Calvaria. ACS Applied Bio Materials, 2020, 3, 7762-7768.	4.6	12
115	Porosity-controllable magnetoplasmonic nanoparticles and their assembled arrays. Nanoscale, 2020, 12, 8453-8465.	5.6	12
116	Molybdenum Trioxide Quantum Dot-Encapsulated Nanogels for Virus Detection by Surface-Enhanced Raman Scattering on a 2D Substrate. ACS Applied Materials & Interfaces, 2021, 13, 27836-27844.	8.0	12
117	Real-time SPR imaging based on a large area beam from a wavelength-swept laser. Optics Letters, 2018, 43, 5476.	3.3	12
118	Surface plasmon resonance spectroscopic chiral discrimination using self-assembled leucine derivative monolayer. Talanta, 2008, 76, 49-53.	5.5	11
119	Solvent Effect in Dynamic Superstructures from Au Nanoparticles and CdTe Nanowires: Experimental Observation and Theoretical Description. Journal of Physical Chemistry C, 2010, 114, 1404-1410.	3.1	11
120	Detection of anti-Neospora antibodies in bovine serum by using spiky Au–CdTe nanocomplexes. Sensors and Actuators B: Chemical, 2013, 178, 192-199.	7.8	11
121	Synthesis of 2D and 3D hierarchical β-FeOOH nanoparticles consisted of ultrathin nanowires for efficient hexavalent chromium removal. Applied Surface Science, 2021, 543, 148823.	6.1	11
122	Highly flexible and transparent metal grids made of metal nanowire networks. RSC Advances, 2015, 5, 77288-77295.	3.6	10
123	Amorphous Ni <sub>1–<i>x</i></sub> Fe <sub><i>x</i></sub> Oxyhydroxide Nanosheets with Integrated Bulk and Surface Iron for a High and Stable Oxygen Evolution Reaction. ACS Applied Energy Materials, 2021, 4, 6833-6841.	5.1	10
124	Uranyl ion detection based on wavelength-resolved surface plasmon resonance spectroscopy. Sensors and Actuators B: Chemical, 2008, 134, 419-422.	7.8	9
125	Nanoassembly of CdTe nanowires and Au nanoparticles: pH dependence and reversibility of photoluminescence. Korean Journal of Chemical Engineering, 2009, 26, 417-421.	2.7	9
126	Cultures of <scp>S</scp> chwann–like cells differentiated from adiposeâ€derived stem cells on <scp>PDMS</scp> / <scp>MWNT</scp> sheets as a scaffold for peripheral nerve regeneration. Journal of Biomedical Materials Research - Part A, 2015, 103, 3642-3648.	4.0	9

#	Article	IF	CITATIONS
127	Highly stable functionalized aluminum nanoparticles for magneto-energetic composite fabrication. Combustion and Flame, 2018, 187, 96-104.	5.2	9
128	Ultrasensitive Fluorescence Monitoring and <i>in Vivo</i> Live Imaging of Circulating Tumor Cell-Derived miRNAs Using Molecular Beacon System. ACS Sensors, 2018, 3, 2651-2659.	7.8	9
129	In Vivo Study of Spiky Fe3O4@Au Nanoparticles with Different Branch Lengths: Biodistribution, Clearance, and Biocompatibility in Mice. ACS Applied Bio Materials, 2019, 2, 163-170.	4.6	9
130	Photonic–Plasmonic Nanostructures for Solar Energy Utilization and Emerging Biosensors. Nanomaterials, 2020, 10, 2248.	4.1	9
131	Au nanozyme-driven antioxidation for preventing frailty. Colloids and Surfaces B: Biointerfaces, 2020, 189, 110839.	5.0	9
132	A surface plasmon resonance study on the optical properties of gold nanoparticles on thin gold films. Mikrochimica Acta, 2011, 172, 489-494.	5.0	8
133	Ligand Exchange Procedure for Bimetallic Magnetic Iron–Nickel Nanocrystals toward Biocompatible Activities. ACS Applied Materials & Interfaces, 2015, 7, 15522-15530.	8.0	8
134	Simultaneous enhancement of Raman scattering and fluorescence emission on graphene quantum dot-spiky magnetoplasmonic supra-particle composite films. RSC Advances, 2015, 5, 81753-81758.	3.6	8
135	<i>In vivo</i> feasibility test using transparent carbon nanotubeâ€coated polydimethylsiloxane sheet at brain tissue and sciatic nerve. Journal of Biomedical Materials Research - Part A, 2017, 105, 1736-1745.	4.0	8
136	Magnetic Layer-by-Layer Assembly: From Linear Plasmonic Polymers to Oligomers. ACS Applied Materials & Interfaces, 2020, 12, 16584-16591.	8.0	8
137	Density Functional Theoretical Study on the Reduction Potentials of Catechols in Water. Bulletin of the Korean Chemical Society, 2012, 33, 3889-3890.	1.9	8
138	Full-Color Laser Displays Based on Optical Second-Harmonic Generation from the Thin Film Arrays of Selenium Nanowires. ACS Photonics, 2022, 9, 368-377.	6.6	8
139	Microfabrication and optical properties of highly ordered silver nanostructures. Nanoscale Research Letters, 2012, 7, 292.	5.7	7
140	Effect of polydiacetylene-based nanosomes on cell viability and endocytosis. Nanotechnology, 2019, 30, 245101.	2.6	7
141	Iron–Palladium magnetic nanoparticles for decolorizing rhodamine B and scavenging reactive oxygen species. Journal of Colloid and Interface Science, 2021, 588, 646-656.	9.4	7
142	Enhanced Internalization of Macromolecular Drugs into Mycobacterium smegmatis with the Assistance of Silver Nanoparticles. Journal of Microbiology and Biotechnology, 2017, 27, 1483-1490.	2.1	7
143	Ammonium Ion Optical Sensor Formation and Characterization of a Selfâ€Assembled Thiazole Containing Dibenzoâ€18â€Crownâ€6 Monolayer toward Developing Ammonium Ionâ€5ensing Interface. Analytical Letters, 2007, 40, 3373-3382.	1.8	6
144	Toxic chemical monitoring of agricultural bioproducts using nanomaterials-based sensors. Korean Journal of Chemical Engineering, 2013, 30, 1825-1832.	2.7	6

Jaebeom Lee

#	Article	IF	CITATIONS
145	WO3–ZnO and CuO–ZnO nanocomposites as highly efficient photoanodes under visible light illumination. Nanotechnology, 2020, 31, 255702.	2.6	6
146	Trends in Diagnosis for Active Tuberculosis Using Nanomaterials. Current Medicinal Chemistry, 2019, 26, 1946-1959.	2.4	6
147	"Cloud―assemblies: quantum dots form electrostatically bound dynamic nebulae around large gold nanoparticles. Physical Chemistry Chemical Physics, 2010, 12, 11878.	2.8	5
148	Optical and electrical nano eco-sensors using alternative deposition of charged layer. Frontiers of Materials Science, 2011, 5, 40-49.	2.2	5
149	Facile synthesis of phase-pure FeCr <sub>2</sub> Se <sub>4</sub> and FeCr <sub>2</sub> S <sub>4</sub> nanocrystals via a wet chemistry method. Journal of Materials Chemistry C, 2014, 2, 3744-3749.	5.5	5
150	Optical Anisotropicity of Coreâ€Shell or Yolkâ€Shellâ€typed Ag@Fe <sub>3</sub> O <sub>4</sub> Nanochains. Bulletin of the Korean Chemical Society, 2018, 39, 1273-1278.	1.9	5
151	Contralateral spreading of substances following intratympanic nanoparticle-conjugated gentamicin injection in a rat model. Scientific Reports, 2020, 10, 18636.	3.3	5
152	Sterilization effects of UV laser irradiation on <i>Bacillus atrophaeus</i> spore viability, structure, and proteins. Analyst, The, 2021, 146, 7682-7692.	3.5	5
153	Antibacterial Activity of Graphene-Based Nanomaterials. Advances in Experimental Medicine and Biology, 2022, 1351, 233-250.	1.6	5
154	Silver-enhanced conductivity of magnetoplasmonic nanochains. Current Applied Physics, 2015, 15, 110-114.	2.4	4
155	Density-Controlled Freestanding Biodegradable Nanopillar Arrays Patterned via Block Copolymer Micelle Lithography. Macromolecular Materials and Engineering, 2017, 302, 1600361.	3.6	4
156	Human Tonsil-Derived Mesenchymal Stem Cells-Loaded Hydroxyapatite-Chitosan Patch for Mastoid Obliteration. ACS Applied Bio Materials, 2020, 3, 1008-1017.	4.6	4
157	<i>In Vivo</i> Study of Mastoid Obliteration Using Hydroxyapatite-Chitosan Patch. Journal of Biomedical Nanotechnology, 2017, 13, 1715-1724.	1.1	4
158	Vertically aligned multi-layered structures to enhance mechanical properties of chitosan–carbon nanotube films. Journal of Materials Science, 2015, 50, 2587-2593.	3.7	3
159	Expandable photo-induced synthetic route to generate highly controlled noble metal nanoparticles. Current Applied Physics, 2015, 15, 1100-1105.	2.4	3
160	Evaluation of <i>β</i> -Amyloid Peptides Fibrillation Induced by Nanomaterials Based on Molecular Dynamics and Surface Plasmon Resonance. Journal of Nanoscience and Nanotechnology, 2015, 15, 1110-1116.	0.9	3
161	Modality switching between therapy and imaging based on the excitation wavelength dependence of dual-function agents in folic acid-conjugated graphene oxides. Biomedical Optics Express, 2018, 9, 705.	2.9	3
162	Chirality of Fingerprints: Pattern- and Curvature-Induced Emerging Chiroptical Properties of Elastomeric Grating Meta-Skin. ACS Nano, 2022, 16, 6103-6110.	14.6	3

#	Article	IF	CITATIONS
163	Effect of surface charge of gold nanoparticles on fluorescence amplification of polydiacetylene-based liposomes. Journal of Experimental Nanoscience, 2020, 15, 174-181.	2.4	2
164	Assembly of Nanomaterials using Polymers and Biomaterials: Sensing and Electronic Applications. Materials Research Society Symposia Proceedings, 2005, 901, 1.	0.1	1
165	Surface Plasmon Resonance Investigation of a Copolymer Containing Spiroxazine. Journal of Nanoscience and Nanotechnology, 2009, 9, 7195-8.	0.9	1
166	Phenylalanine Sensing Based on Surface Plasmon Resonance. Journal of Nanoscience and Nanotechnology, 2009, 9, 7199-203.	0.9	1
167	Thermal behavior of surface plasmon resonance in dynamic suprastructure multilayer. Current Applied Physics, 2013, 13, 940-944.	2.4	1
168	Electrochemical Investigation of Porosity in Core–Shell Magnetoplasmonic Nanoparticles. Journal of Physical Chemistry Letters, 2022, 13, 6085-6092.	4.6	1
169	Fluorescence enhancement and energy transport from bioconjugation between nanowires and nanoparticles. , 2004, , .		0
170	Photoluminescence Up-Conversion of Bioconjugated Hybrids on CdTe and Au Nanoparticles. Journal of Nanoscience and Nanotechnology, 2009, 9, 7061-4.	0.9	0
171	Real-time deformation monitoring of sol-gel-induced SiO2-TiO2 films using laser-induced fluorescence microscopy for corrosion protection. Korean Journal of Chemical Engineering, 2011, 28, 1770-1772.	2.7	0
172	Nanotechnology: A New Approach to Improve Orthopedic Implants. , 2012, , 401-443.		0
173	Metal-Enhanced Fluorescence and Ultrafast Energy Transfer of Dyes near Silver Nanosurfaces. ACS Symposium Series, 2016, , 209-225.	0.5	0